Original Article

Electronic, spectroscopic, and vibrational properties of Si diamondoid nanocrystals: An LSDA study

Mudar Ahmed Abdulsattar*, A. J. Hashim, Mohammed E. Ismael

Ministry of Science and Technology, Baghdad, Iraq.

Correspondence: Mudar Ahmed Abdulsattar, Ministry of Science and Technology, Baghdad, Iraq.

ABSTRACT

Stable Si diamondoids are used to investigate Si nanocrystals and as an approach to Si bulk properties using local spin density approximation (LSDA). HOMO, LUMO, energy gap of Si diamondoids, size variation, and the effect of nanocrystals shape are all investigated. Vibrational force constant of Si diamondoids reaches 0.95 mDyne/Å. This value is lower than bulk silicon. Si-Si vibrational frequency reaches 502.9 cm^{-1}, and vibrational reduced mass reaches 14.2 amu. These two quantities are higher than the values of bulk Si. UV-Vis spectra show the movement of the peak from 114 nm to nearly 281.5 nm with increasing size of Si diamondoids. This trend of values is compared with experimental Si quantum dots at 440 nm. NMR spectra are shown that it can differentiate between different Si molecules and diamondoids as a function of size. All Si diamondoids properties are sensitive to Si diamondoids size. NBO population analysis displays that investigated molecular bonding deviates from sp^3 bonding. The bonding of Si valence orbitals is in the extent ([core]$3s^{1.17}3p^{2.89}3d^{0.02}4p^{0.01}$ to [core]$3s^{1.16}3p^{2.68}3d^{0.01}$) depending on the location of Si atom.

Keywords: DFT; Nanocrystals; Vibration; UV-Vis; NMR

Introduction

Silicon is a critical semiconductor in the nanoscale range [1]. The energy gap of bulk Si is 1.12 eV. This gap is expanded as we arrive at the nanoscale quantum confinement region [2]. Expanding the Si gap will end in a gap that can cross the visible range. Silicon alloying with other elements such as other group IV elements can change the gap value to a wide range of values. Current uses of Si nanoclusters include electronics [3], photonics [4], solar cells [5], and gas sensors [6].

Access this article online	
Website: www.japer.in	**E-ISSN:** 2249-3379

How to cite this article: Mudar Ahmed Abdulsattar, A. J. Hashim, Mohammed E. Ismael. Electronic, spectroscopic, and vibrational properties of Si diamondoid nanocrystals: An LSDA study. J Adv Pharm Educ Res. 2020;10(3):82-9.
Source of Support: Nil, Conflict of Interest: None declared.

Diamondoids are cage-like stable molecules originated in natural petroleum. These diamondoids have several properties that make them very similar in many ways to the diamond and zinc-blend bulk-structure materials. Diamondoid structures are found feasible at least theoretically for C, Si, Ge, and Sn. It is also feasible for zincblende structure materials [7, 8]. Both carbon and smallest silicon diamondoids are manufactured in the lab [7]. Hydrogen is usually important to stabilize diamondoids' surface. Non-passivated Si clusters [9, 10] have different electronic structure than the sp^3 orbital bonding at least on their surface. This results in a smaller HOMO-LUMO gap and binding energy of bare Si clusters because of dangling surface bonds. The purpose of the current investigation was to explore the size-dependent variation of different spectroscopic properties of Si diamondoids. The importance of this goal can be realized from the growing literature and applications of the present diamondoids [2-10].

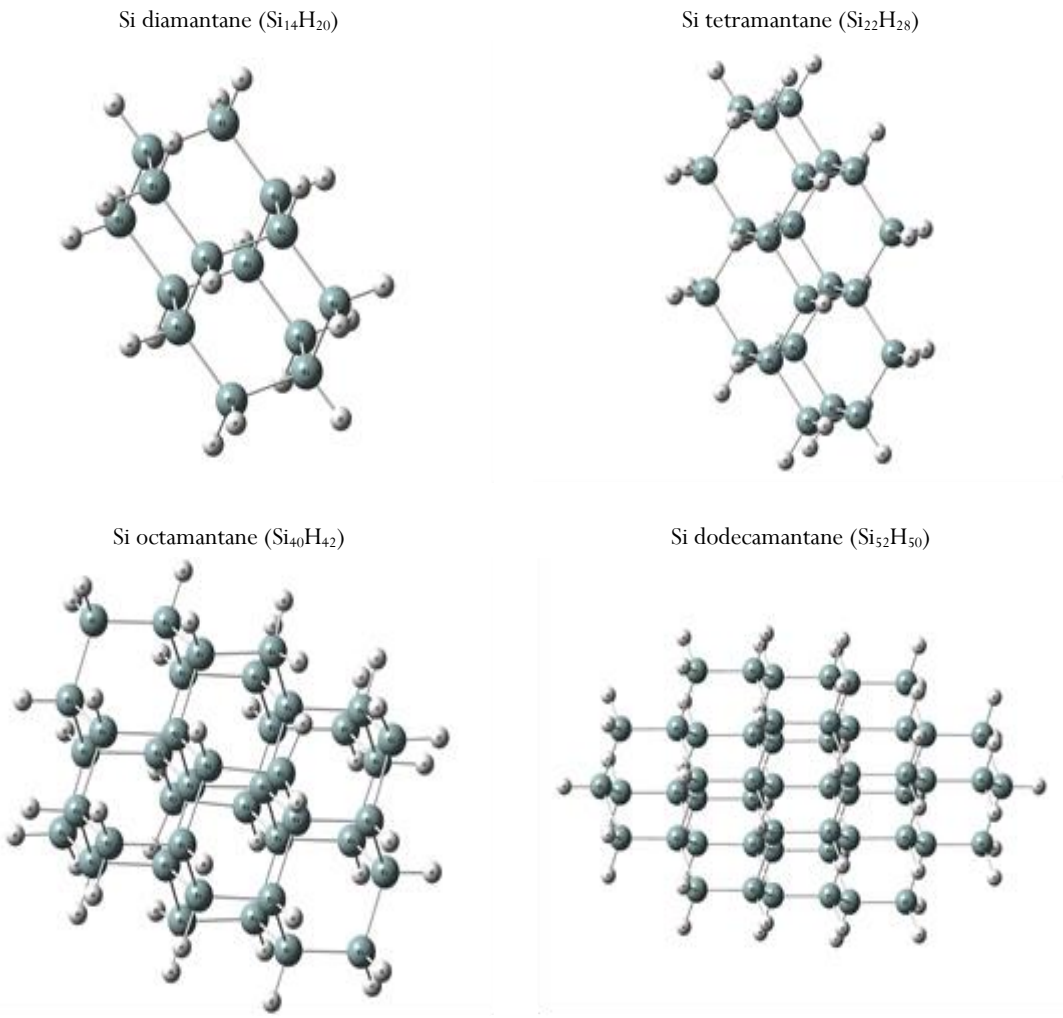

Figure 1: Some Si diamondoid molecules with optimized structures.

Theory

After scanning several density functional theories (DFT), we arrived at choosing local spin density approximation (LSDA). The same is true for choosing suitable basis functions. Basis functions are also scanned for being convenient for the present type of calculations. We ended at choosing 6-311G** basis functions that are suitable in terms of accuracy, time, and resource consumption. The benchmark of our tests was the energy gap. The scanned theories included LSDA, PBE, and B3LYP. The experimental data of the energy gap for carbon adamantane is 6.492 eV [11]. Theoretically calculated energy gaps were compared to arrive at the selected theory and basis states mentioned above [12, 13].

The smallest investigated molecules in the present study were disilane (Si_2H_6) and Si cyclohexane (Si_6H_{12}). Although these are non-diamondoid molecules, they serve as building blocks of diamondoids themselves. Si-adamantane ($Si_{10}H_{16}$) is the smallest Si-diamondoid. Other investigated Si diamondoids comprised Si diamantane ($Si_{14}H_{20}$), Si triamantane ($Si_{18}H_{24}$), Si tetramantane ($Si_{22}H_{28}$), Si pentamantane ($Si_{26}H_{32}$), Si hexamantane ($Si_{26}H_{30}$), Si octamantane ($Si_{40}H_{42}$), and Si dodecamantane ($Si_{52}H_{50}$). Fig (1) lists some of the investigated Si diamondoids. The dimensions of Si octamantane ($Si_{40}H_{42}$) and Si dodecamantane ($Si_{52}H_{50}$) exceeds 1 nm of length.

Spectroscopic properties such as NMR, vibrational analysis, and UV-Vis were calculated. Vibrational frequencies were corrected using 0.988 scale factor that corresponds to the present theory and basis (LSDA/6-311G**) [12]. Gaussian09 suite of programs was used to perform the present calculations [14].

Results and Discussion

Energy gap, HOMO, and LUMO variation with the number of Si atoms are shown in Fig (2). Experimental bulk limit of energy gap is shown as a dashed line at the value 1.12 eV [1]. The results are in agreement with the confinement theory foundations. The non-spherical shape of Si diamondoids results in fluctuations in the energy gap [15, 16]. Some of the Si clusters such as $Si_{126}H_{92}$ in Figs (2) and (8) are very close to being spherical. HOMO level fluctuations are the cause of the variable energy gap. The energy gap of the bare Si clusters is lower than the experimental gap due to the surface dangling bonds. An example of this situation is bare Si diamantane cluster that has an energy gap of 0.45 eV compared to 4.87 eV for hydrogen surface passivated Si diamantane.

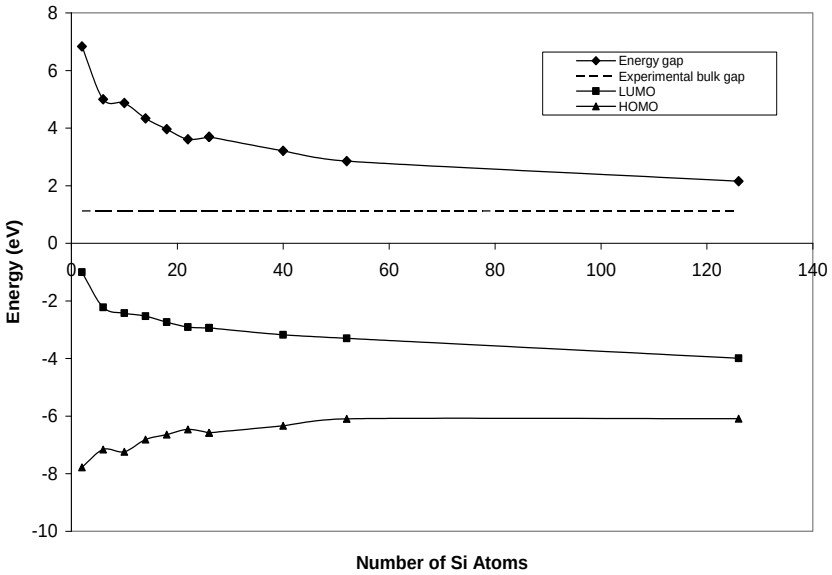

Figure 2: Energy gap, HOMO, and LUMO changes with the number of Si atoms. The bulk experimental gap is represented by a dashed line having a value of 1.12 eV [2].

Two methods can be used to analyze vibrational modes. The first one depends on the reduced masses and the second one depends on force constants. The first one is much easier since the masses of atoms are better known than vibrational force constants. As an example, when the reduced mass is very near to one, the vibration is mainly due to a hydrogen atom. If the vibration reduced mass is very near to 14, then the vibration is due to two silicon atoms (Si atomic mass is 28 amu). This can be manifested in Figs (3) and (4). Si disilane and Si hexamantane force constant and the reduced mass as a function of vibrational frequency are shown. The first main distinguished region of vibration is from 0-503 cm^{-1}. Both reduced mass and force constant are fluctuating in this region. The highest force constant in this region starts by the value of 0.75 mDyne/Å for disilane and 0.95 mDyne/Å for Si hexamantane. These values are less than bulk carbon (4.7 mDyne/Å) and bulk silicon (2.4 mDyne/Å) [17, 18]. The longitudinal optical (LO) mode corresponds to the highest force constant mode (HFCM) [19, 20]. The highest reduced mass mode (HRMM) is 6.8 amu for disilane and 14.26 amu for Si hexamantane. The reduced mass of Si hexamantane is nearly equal to the reduced mass of two silicon atoms (14 amu). H atoms vibrate in the second region against the whole cluster of silicon atoms. As a result, the reduced mass of such vibration is equal to one since the hydrogen mass is much lower than the mass of the cluster. The frequency of HFCM increases from 426.5 cm^{-1} for disilane to 502.94 cm^{-1} for Si hexamantane. This last value approaches that of bulk Si (520 cm^{-1}) [21]. The second part of Fig (3) includes H scissor vibrations at 855 cm^{-1}. Symmetric and asymmetric vibrations are at 2100 cm^{-1}.

$Si_{22}H_{28}$ and $Si_{26}H_{30}$ have lower UV-Vis intensity relative to non-diamondoids (Si_2H_6 and Si_6H_{12}) as shown in Fig (5). The crest maximum in UV-Vis spectra moves from 114.5 nm for disilane to 280 nm for Si hexamantane. The last value is heading towards experimental value for Si quantum dots at 440 nm [22].

Fig (6) shows the results of the natural bond orbital analysis (NBO). The charges on each Si atom depends on the number of H atoms attached to it. The hydrogen atoms bear negative charges since they have higher electron affinity than Si atoms. The bonding orbitals are in the range [core]$3s^{1.17}3p^{2.893}d^{0.024}p^{0.01}$ to [core]$3s^{1.16}3p^{2.68}3d^{0.01}$. The surface bonding configuration [core]$3s^{1.16}3p^{2.68}3d^{0.01}$ that is equal to a total electronic charge of 3.85 a.u. Group IV elements manage to hybridize orbitals towards free atom hybridization of s^2p^2 [23].

Electronic spin creates a magnetic field contrasting the magnetic field produced by the nuclear constituents. Fig (7) shows a variation of ^{1}H-NMR of Si diamondoids. The ^{1}H-NMR lines are confined between the minimum and maximum lines shown in this figure. The first point in Fig (7) that represents disilane displays a coincidence between the minimum and maximum ^{1}H-NMR lines because of symmetry. Non-Diamondoids molecules show shielding values that are higher than diamondoids in Fig (7). The binding energy of Si diamondoids and molecules per Si atom is shown in Fig (8). These values were compared with the bulk experimental value of 4.7 eV [23]. The surface H atoms increase this value over the experimental one. However, this increment decreases gradually as the number of atoms increases and the surface to bulk ratio decreases. The binding energy of bare and hydrogen passivated Si diamantane are 5.4 and 9.8 eV, respectively. Spectroscopic properties, energy gap, binding energy, bond lengths, etc. are compatible with the series of values found for group IV elements [23-26]. All the calculated spectroscopic properties are important in Si nanocluster applications [3-6] and the quality of Si nanoclusters simulation is vitally connected to these structures' particle size, vibrational frequencies, NMR, and UV-Vis [27].

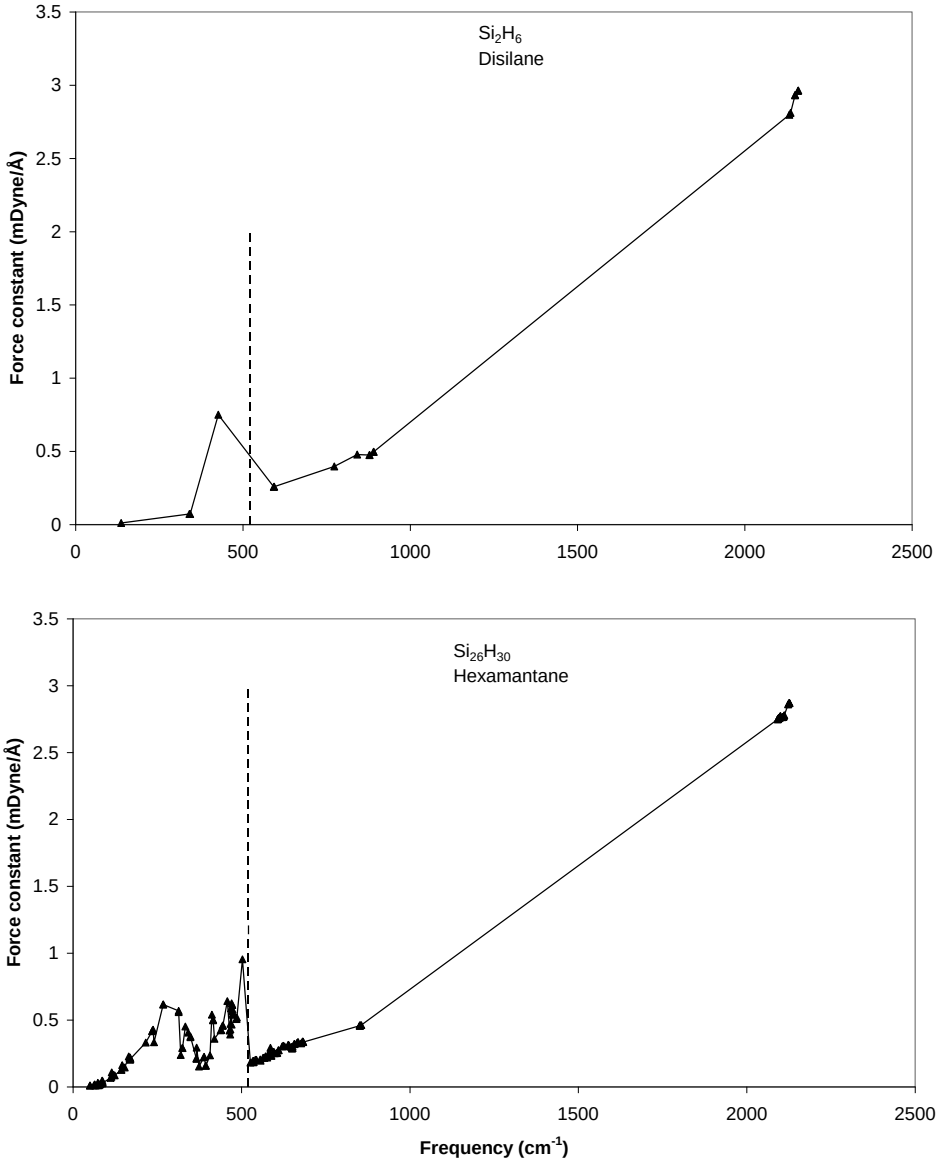

Figure 3: Vibration force constants for disilane and Si hexamantane as a function of frequency (cm^{-1}). Experimental LO mode bulk value frequency [20] are shown for comparison.

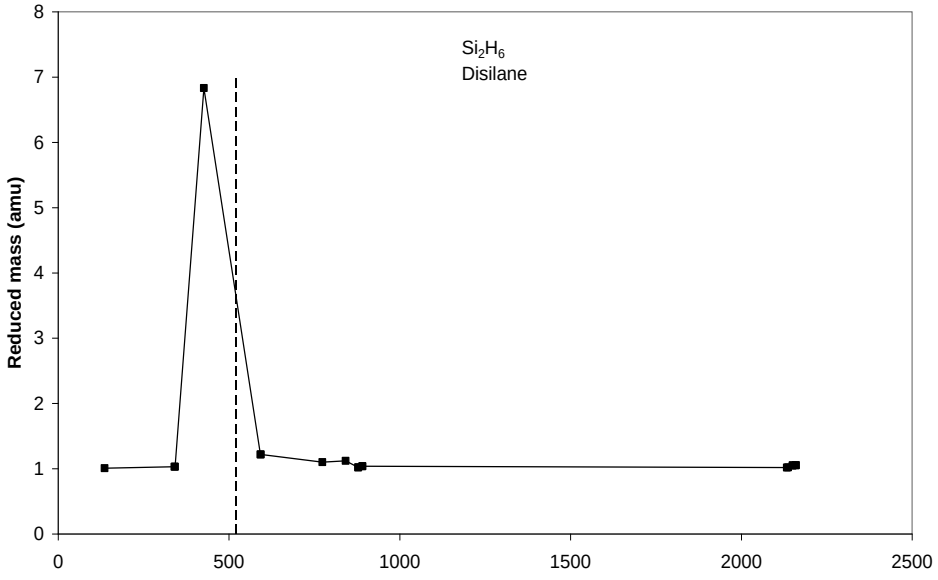

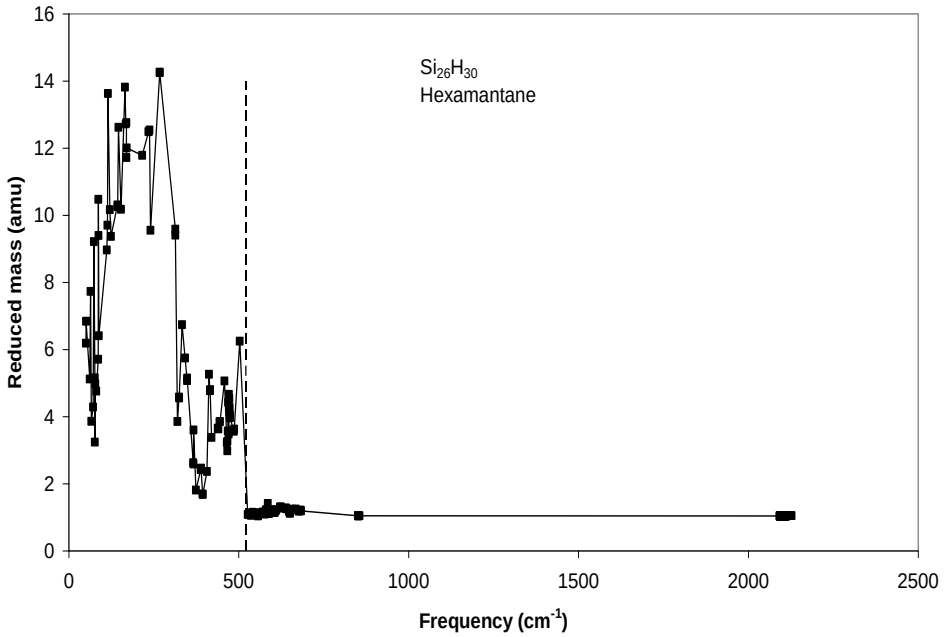

Figure 4: Vibrational reduced masses for disilane and Si hexamantane as a function of frequency (cm^{-1}). Experimental LO mode bulk value [20] are shown for comparison.

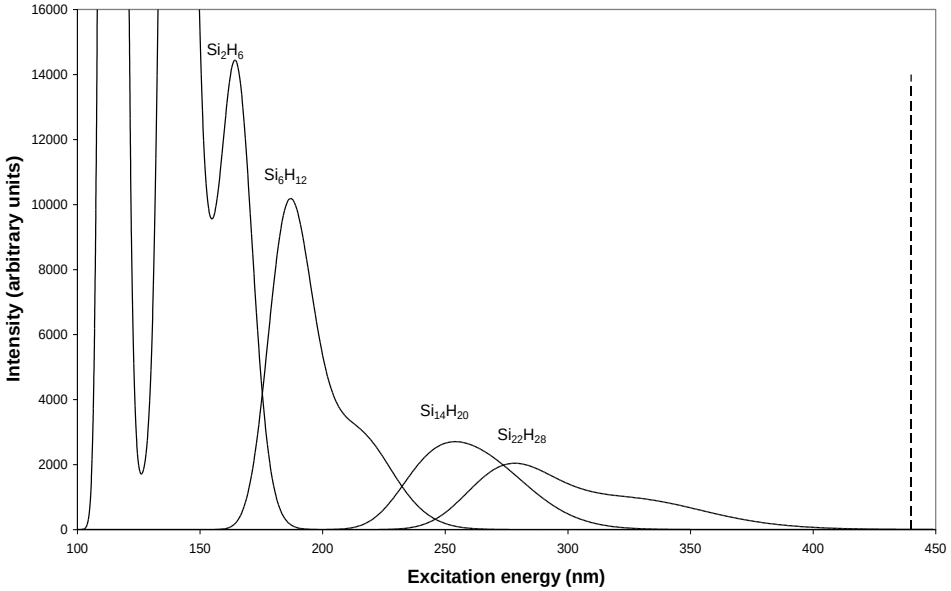

Figure 5: UV-Vis in terms of excitation energy for hydrogen passivated Si molecules and diamondoids. UV-Vis Experimental bulk value of Si quantum dots is shown for comparison [21].

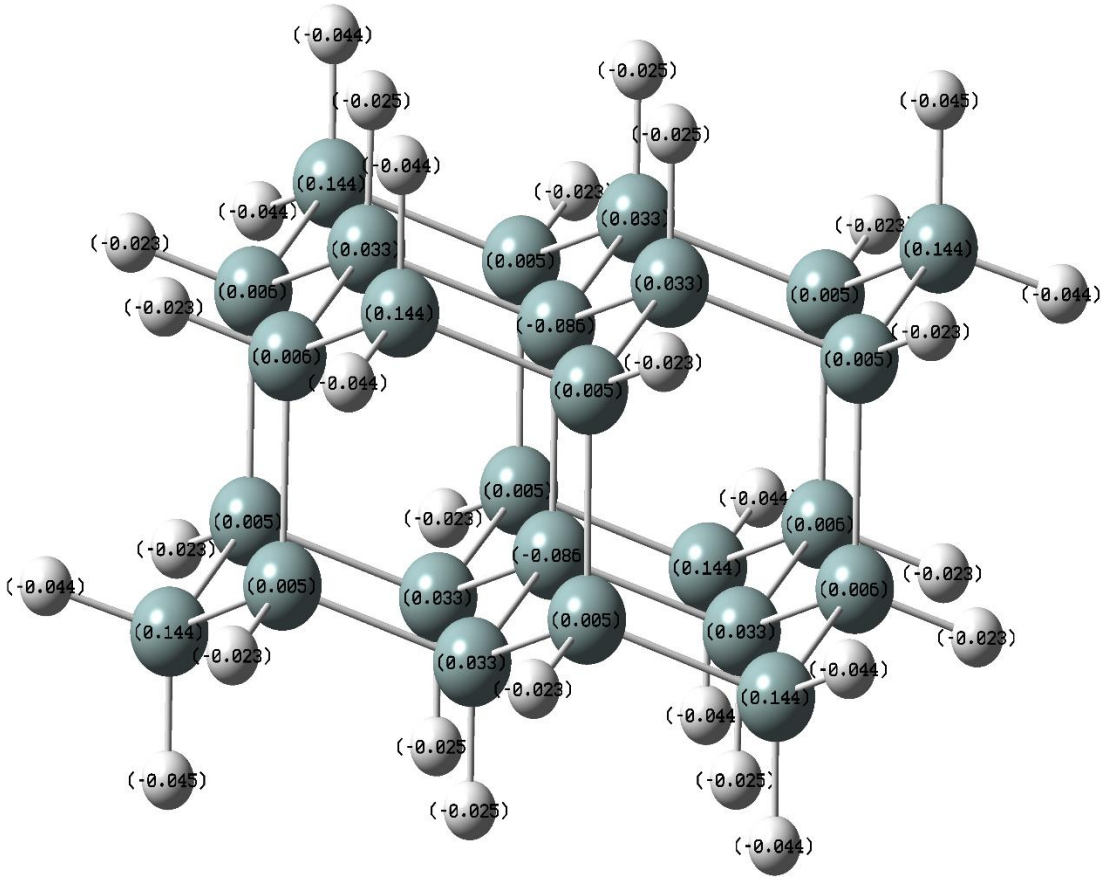

Figure 6: Atomic charges in Si hexamantane according to NBO analysis.

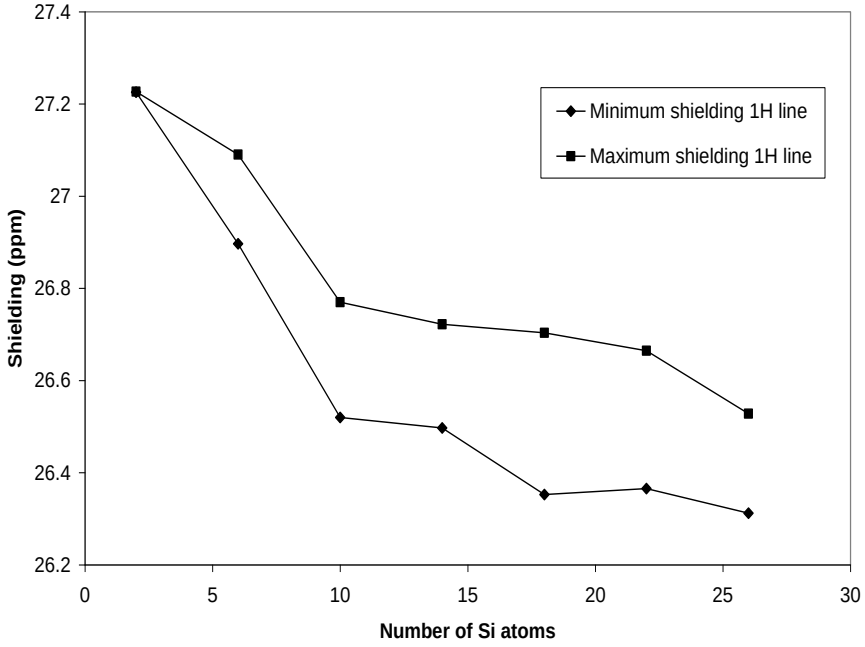

Figure 7: Min and max ^{1}H-NMR shielding of Si molecules and diamondoids.

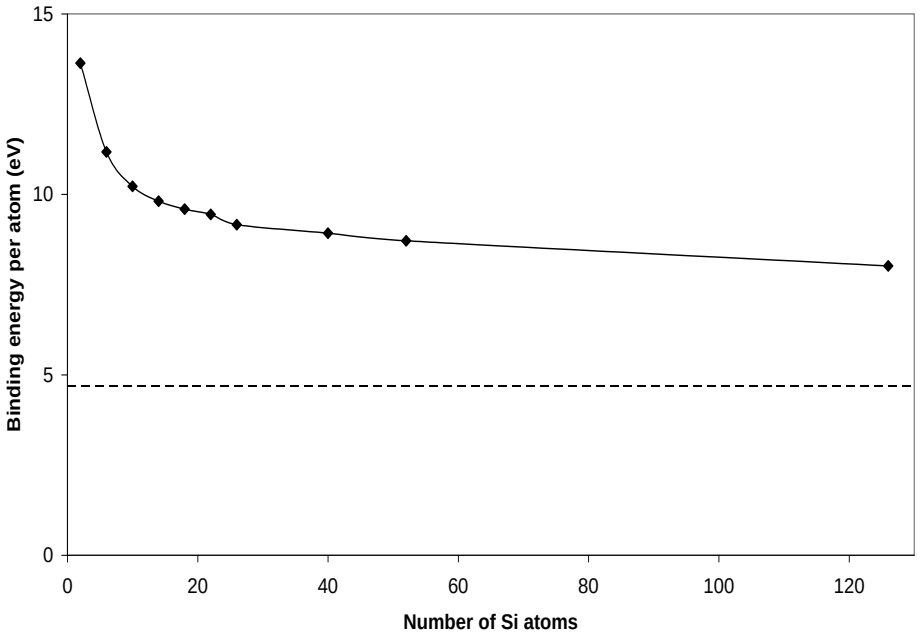

Figure 8: Binding energy per Si atom for investigated Si molecules and diamondoids. Experimental binding energy bulk value is shown for comparison [22].

Conclusions

Si molecules and diamondoids, discussed in the present work have properties that can discriminate between them and also discriminate them from bulk. These investigated properties include energy gap, vibrational spectra, UV-Vis, and ^{1}H-NMR. All these properties refer to higher stable structures. As an example, UV-Vis intensity of Si diamondoids is lower than Si molecules. Another example is Si diamondoids smaller relative ^{1}H-NMR shielding than Si molecules. As the number of Si atoms increases, all Si diamondoids properties manage to converge to Si bulk values. This convergence is approached in a different way than the usual Si molecules. As an example, the binding energy per Si atom tends to be much higher because of the existence of hydrogen surface atoms.

References

1. Eghbali Borujeni A. Investigation of the Magnetic, Electronic and Structural Properties of Nickel, Cobalt, and Iron Thin Layers on Silicon (001) Substrate. World J Environ Biosci, 2018;7(1):75-8.
2. Lu H, Zhao YJ, Yang XB, Xu H. Theoretical investigation of structural stability and electronic properties of hydrogenated silicon nanocrystals: Size, shape, and surface reconstruction. Physical Review B. 2012 Aug 22;86(8):085440.
3. Singh IV, Alam MS. Analog/RF Performance Investigation of Nanoscale Gate-Underlap Single and Double Gate Silicon-On-Insulator MOSFETs with High-k Stack on Spacer. Journal of Nanoelectronics and Optoelectronics. 2015 Dec 1;10(6):790-4.
4. Thévenaz L. Silicon nanophotonics: Good vibrations for light. Nature Photonics. 2015 Mar;9(3):144-6.
5. Savin H, Repo P, Von Gastrow G, Ortega P, Calle E, Garín M, Alcubilla R. Black silicon solar cells with interdigitated back-contacts achieve 22.1% efficiency. Nature nanotechnology. 2015 Jul;10(7):624-8.
6. Peng S, Ming H, Mingda L, Shuangyun M. Nano-WO3 film modified macro-porous silicon (MPS) gas sensor. Journal of Semiconductors. 2012 May;33(5):054012.
7. Fischer J, Baumgartner J, Marschner C. Synthesis and structure of sila-adamantane. Science. 2005 Nov 4;310(5749):825-.
8. Ramachandran G, Manogaran S. Vibrational spectra of triamantane X18H24, iso-tetramantane X22H28 and cyclohexamantane X26H30 (X= C, Si, Ge, Sn)–a theoretical study. Journal of Molecular Structure: THEOCHEM. 2007 Aug 20;816(1-3):31-41.
9. Marsen B, Lonfat M, Scheier P, Sattler K. The energy gap of pristine silicon clusters. Journal of Electron Spectroscopy and Related Phenomena. 2000 Aug 1;109(1-2):157-68.
10. Haertelt M, Lyon JT, Claes P, de Haeck J, Lievens P, Fielicke A. Gas-phase structures of neutral silicon clusters. The Journal of chemical physics. 2012 Feb 14;136(6):064301.
11. Landt L, Klünder K, Dahl JE, Carlson RM, Möller T, Bostedt C. Optical response of diamond nanocrystals as a function of particle size, shape, and symmetry. Physical review letters. 2009 Jul 23;103(4):047402.
12. NIST Computational chemistry comparison and benchmark database, release 15b, 2011. http://cccbdb.nist.gov/ (accessed Dec 1, 2014).

13. Willey TM, Bostedt C, Van Buuren T, Dahl JE, Liu SG, Carlson RM, Meulenberg RW, Nelson EJ, Terminello LJ. Observation of quantum confinement in the occupied states of diamond clusters. Physical Review B. 2006 Nov 28;74(20):205432.
14. Frisch MJ, Trucks GW, Schlegel HB, Scuseria GE, Robb MA, Cheeseman JR, Scalmani G, Barone V, Mennucci B, Petersson G, Nakatsuji H. Gaussian 09, revision a. 02, gaussian. Inc., Wallingford, CT. 2009 Jun 11;200:28.
15. Abdulsattar MA, Sultan TR, Saeed AM. Shape and size dependence of electronic properties of InSb diamondoids and nanocrystals: a density functional theory study. Advances in Condensed Matter Physics. 2013;2013.
16. Abdulsattar MA, Mohammed IS. Diamondoids and large unit cell method as building blocks of InAs nanocrystals: A density functional theory study. Computational Materials Science. 2014 Aug 1;91:11-4.
17. Abdulsattar MA, Majeed SA, Saeed AM. Electronic, Structural, and Vibrational Properties of α-Sn Nanocrystals Built From Diamondoid Structures: Ab InitioStudy. IEEE Transactions on Nanotechnology. 2014 Aug 26;13(6):1186-93.
18. Schrader B. (ed) Infrared and Raman spectroscopy. VCH Verlagsgesellschaft mbH, Weinheim.1995.
19. Abdulsattar MA. Size dependence of Si nanocrystals infrared spectra: A density functional theory study. Silicon. 2013 Jul 1;5(3):229-37.
20. Abdulsattar MA. Size variation of infrared vibrational spectra from molecules to hydrogenated diamond nanocrystals: a density functional theory study. Beilstein journal of nanotechnology. 2013 Apr 15;4(1):262-8.
21. Gupta R, Xiong Q, Adu CK, Kim UJ, Eklund PC. Laser-induced Fano resonance scattering in silicon nanowires. Nano Letters. 2003 May 14;3(5):627-31.
22. Yi Y, Deng J, Zhang Y, Li H, Yao S. Label-free Si quantum dots as photoluminescence probes for glucose detection. Chemical Communications. 2013;49(6):612-4.
23. Abdulsattar MA, Al-Bayati KH. Corrections and parametrization of semiempirical large unit cell method for covalent semiconductors. Physical Review B. 2007 Jun 7;75(24):245201.
24. Wen B, Zhao J, Li T. Relative stability of hydrogenated nanodiamond and nanographite from density function theory. Chemical physics letters. 2007 Jun 25;441(4-6):318-21.
25. Zhuang C, Jiang X, Zhao J, Wen B, Jiang X. Infrared spectra of hydrogenated nanodiamonds by first-principles simulations. Physica E: Low-dimensional Systems and Nanostructures. 2009 Aug 1;41(8):1427-32.
26. Samizadeh M, Ebrahimi M, Pordel M. Preparation of Molecularly Imprinted Polymers Coupled with Magnetic Nanoparticles for the Selective Extraction of Propranolol from Aqueous Solution of Propranolol, Atenolol and Metoprolol. Journal of Biochemical Technology. 2018;9(4):22.
27. Manojkanna K, Chandana CS. Nanoparticles in endodontics–A review. J Adv Pharm Edu Res 2017;7(2):58-60.